Int. J. on Recent Trends in Engineering and Technology, Vol. 9, No. 1, July 2013

Optimal Control of a Teleoperation System via LMI-based Robust PID Controllers

A. Roushandel [1], A. Alfi [2], and A. Khosravi [3]
[1] Babol University of Technology/ Electrical and Computer Engineering Department, Babol, Iran
Email: a.roushandel@stu.nit.ac.ir
[2] Shahrood University of Technology / Electrical and Robotic Engineering Department, Shahrood, Iran
Email: a_alfi@shahroodut.ac.ir
[3] Babol University of Technology / Electrical and Computer Engineering Department, Babol, Iran
Email: akhosravi@nit.ac.ir

***Abstract*—Since the performance of the teleoperation systems can be considerably degraded by time-delay of communication channels and uncertainty in various parts of such systems, the main objectives of the controller design in loads of different structures of the bilateral teleoperation system are to preserve stability and tracking performance of these systems in spite of aforementioned sources of uncertainty. In this paper, a new robust PID controller will be designed based on H_∞ control theory by using the Linear Matrix Inequality (LMI) approach. Therefore, the problem of a Robust PID controller design can be regarded as a special case of the output-feedback controller via employing some sorts of changes in control and system parameters. To show the effectiveness of the proposed controller, the robust PID controller is compared with the multiobjective H_2/H_∞ one. The main feature of the suggested structure is its ability to control the teleoperation system via using the simplest structure in which two signals will be transmitted to control the teleoperation system. In addition, use of PID controller has more practical applications in industrial units, due to its simplicity in implementation and capability to predict the time responses caused by changes in control parameters.**

***Index Terms*— Teleoperation systems, Robust LMI based PID controller, Multiobjective H_2/H_∞, Optimization.**

I. Introduction

There has been a considerable growth in use of teleoperation systems in different areas such as: telesurgery, telemanipulation, space mission, nuclear power station, under sea research, Etc. A typical bilateral teleoperation system depicted in fig. 1 consists of five important parts: a human operator, a master manipulator, communication channels, a slave manipulator and remote environment. The master manipulator is directly drawn by the human operator and its position/velocity is transmitted to the slave site via communication channel. The slave manipulator has to track the position/velocity of master one and communicate reactions of the remote (task) environment to the master manipulator as the reflected force.

Although using the bilateral structure in teleoperation systems increases ability of the human operator to control the teleoperation system, if there was a long distance between slave and master sites, performance and stability of the overall system would be deeply affected. The performance of a teleoperation system is addressed by an index called transparency. Transparency is defined as a match between forces that is exerted by the human operator and one which is reflected from the task environment. In other words, transparency is a capability of a teleoperation system to represent unchanged dynamics of the remote environment to the human operator [1]. Because of the existing uncertainties in dynamics of the system and time-delay in communication channels a compromise is required to be ensured between transparency and stability [2]. Since an increase in stability margins of the system leads to a decrease in transparency, control of a bilateral teleoperation system requires a delicate trade-off between two foregoing requirements namely transparency and robust stability.

Until now several control schemes have been applied to bilateral teleoperation systems so next some of these schemes are considered briefly. H_∞ control theory was used by Sano et al. in 2000 [3]. They used four sensors in order to measure positions and forces of master and slave systems. In 2002, a new control method consisting of smith predictor and wave variables was proposed by Ganjefar et al. [4] for optimizing the performance of the teleportation system against the large variable time-delay. An optimal H_2 procedure was proposed for teleportation systems in 2004 by Boukhnifer and Ferreira [5]. Sunny et al. [6] designed an adaptive position and force stabilizing controller for bilateral teleportation system in 2005. In the same year Ganjefar and Miri [7] used optimization control method in teleportation systems. One year after that, ShaSadeghi et al. [8] proposed a new control structure based on adaptive inverse method while at this year Sirouspoor and Shahdi [9] employed predictor controller for teleportation systems. Tavakoli et al. suggested a modeling and stability analysis for discrete teleoperation system in 2008 [10]. While a sliding mode bilateral control was proposed by Moreau et al. for Master-Slave pneumatic servo systems [11]. Novel adaptive-based methods have been dedicated to various structures of teleoperation systems [12-15] to reduce the destructive effects of time delay and uncertainty on performance of these systems. Additionally, different disturbance based methods have been proposed for bilateral teleoperation systems to preserve the stability and performance [16-18].

DOI: 01.IJRTET.9.1.513

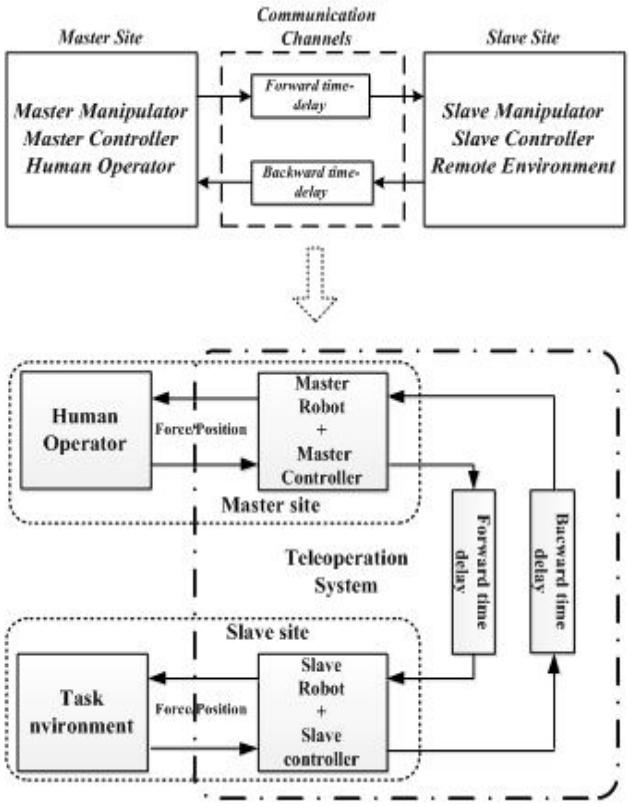

Figure 1. General structure of the bilateral teleoperation system

Recently, LMI-based approaches have been employed to deal with stability and performance problems [19]. In 2008, an LMI approach was proposed to design robust H_∞ and L_1 controllers for bilateral teleoperation systems by M. ShaSadeghi et al. [20]. A teleoperation system with asymmetric time-delays was also studied in the form of LMI [21] in 2009. The stability condition based on LMI has been used to optimize the maximum permitted value of time-delay. The major shortage of the above papers is that the complete transparency has not been achieved.

This paper presents a novel method to design a robust PID controller based on an LMI approach to control a bilateral teleoperation system with uncertainty in large time-delay and parameters of the slave and remote environment. The main objectives of the controller design are to achieve complete transparency and robust stability simultaneously for the closed-loop system. The proposed method consists of two local controllers. One controller is placed on the remote site called slave controller and has to be responsible for tracking the commands of the master system. Referring to the uncertainty in remote site, a new robust PID controller is supposed to be used in the remote site. The second LMI based robust PID controller which is called master controller is positioned on the local site to be in charge of transparency and stability of the Closed-loop. In order to show the effectiveness of the designed controller the simulation results will be compared with the conventional multiobjective H_2/H_∞ controller.

The paper is organized as follows: modeling of the teleoperation system and time-delay of communication channel will be introduced in section 2. Section 3 is devoted to the design of the local controllers. Moreover, the stability analysis of the proposed structure is described at this section. The simulation results will be shown in section 4. And finally, section 5 draws conclusions and some suggestions for the future work must be given.

II. Modeling Of The Teleoperation System

Fig. 2 shows an especial structure [22] of the bilateral teleoperation system that uses direct force-measurement at the remote site. In this Figure *G*, *C* and *y* denote the transfer function of local systems, local controllers, and positions of the local manipulators, respectively. Moreover, the subscripts *m* and *s* is designated to components of the master and slave sites, respectively. T_{ms} and T_{sm} denote the forward and the backward time-delay, whereas K_p, K_f are position and force scaling factors. Z_e is the impedance of the task environment. In addition, F_h, F_e, F_s, F_m are the human operator, task environment and input forces applied to the slave and master by their local controllers, and also F_r is the reflected force from task environment. Finally, *v* represents the sensor noise of the force measurement in the remote site. It is worth noting that due to use of direct force measurement in considered control structure, force sensors are demanded to be used. Hence, the noise of measurement sensor in the remote site should be considered. This force feedback from remote environment makes it easier to control a typical bilateral teleoperation system through providing a better perception and insight about the remote environment for the human operator. This feedback channel, however, may simply lead to instability of teleoperation system with regard to increase in amount of time-delay.

A. Modeling of the manipulators

One degree of freedom teleoperation system has been used for modeling of bilateral teleoperation systems in several literatures [23]. So dynamics of the master and slave manipulators can be described by the state space representation of (1).

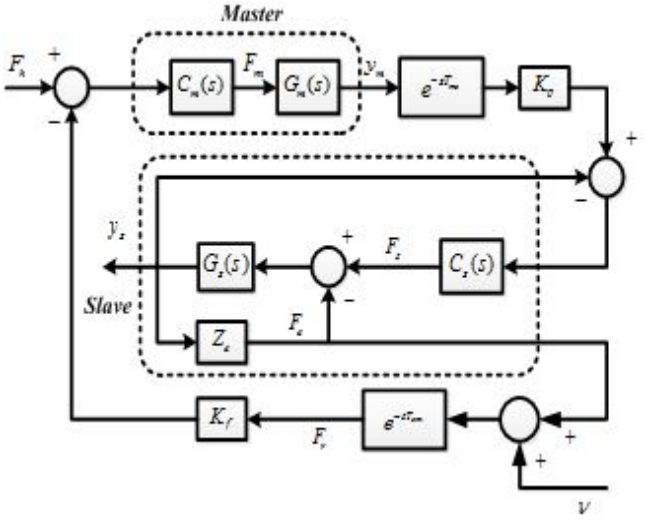

Figure 2. Special Structure of teleoperation system

DOI: 01.IJRTET.9.1.513

In (1), M_j, B_j are inertia and damping coefficients of the manipulators and j=s, m is designated to the slave and master respectively. In state space representation of the robots x_1 and x_3 are the velocities of the master and slave manipulators whereas x_2, x_4 are the positions of the master and slave manipulators. Additionally, f_m and f_s are the input forces of the controllers that will be exerted to the manipulators in order to make desired changes in positions/velocities of them.

$$\begin{aligned}
&\begin{pmatrix}\dot{x}_1\\ \dot{x}_2\end{pmatrix}=\begin{pmatrix}-B_m/M_m & 0\\ 1 & 0\end{pmatrix}\begin{pmatrix}x_1\\ x_2\end{pmatrix}+\begin{pmatrix}1/M_m\\ 0\end{pmatrix}f_m\\
&y_m=\begin{pmatrix}0 & 1\end{pmatrix}\begin{pmatrix}x_1\\ x_2\end{pmatrix}\\
&\begin{pmatrix}\dot{x}_3\\ \dot{x}_4\end{pmatrix}=\begin{pmatrix}-B_s/M_s & 0\\ 1 & 0\end{pmatrix}\begin{pmatrix}x_3\\ x_4\end{pmatrix}+\begin{pmatrix}1/M_s\\ 0\end{pmatrix}\left(f_s-f_e\right)\\
&y_s=\begin{pmatrix}0 & 1\end{pmatrix}\begin{pmatrix}x_3\\ x_4\end{pmatrix}\\
&\underline{M}_s\le M_s\le\bar{M}_s\\
&\underline{B}_s\le B_s\le\bar{B}_s
\end{aligned}\qquad(1)$$

B. Modeling of the communication time-delay

It is worth regarding that the forward T_{ms} and backward T_{sm} time-delays are assumed to be bounded and not necessary identical. By assuming T= T_{ms}+T_{sm}, T can be represented by the signal-flow model [24], [25] as follows:

$$\begin{aligned}
&T=\frac{\left(T_{\max}+T_{\min}\right)}{2}+\frac{\left(T_{\max}-T_{\min}\right)\beta}{2}=\\
&T_{\max}\left(\frac{\left(T_{\max}+T_{\min}\right)}{2T_{\max}}+\frac{\left(T_{\max}-T_{\min}\right)\beta}{2T_{\max}}\right)=\\
&T_{\max}\left(\left(1-\frac{\left(T_{\max}-T_{\min}\right)}{2T_{\max}}\right)+\frac{\left(T_{\max}-T_{\min}\right)\beta}{2T_{\max}}\right)=\\
&T_{\max}\left(1-\theta+\theta\beta\right)=\left(1-\theta\right)T_{\max}+\theta\beta T_{\max}
\end{aligned}\qquad(2)$$

Where β and θ=*(*T_{max}-T_{min}*)/(2*T_{max}*)* are real parameters such that -1d"βd"1 and 0d"θd"0.5. Moreover, T_{max} and T_{min} are the upper and lower bound for the time-delay respectively. When β varies between -1 to 1, the time-delay takes the values between its minimum and maximum values and if T_{min}=*0*, θ=*0.5*. By using the Laplace transformation, the time-delay in (2) can be shown in frequency domain and approximated by the first-order Pade of (3).

$$\begin{aligned}
&e^{-sT}=e^{-s(1-\theta)T_{\max}}.e^{-s\theta\beta T_{\max}}\cong\frac{1-sT/2}{1+sT/2}\\
&\approx\left(\frac{1-s\left(1-\theta\right)T_{\max}/2}{1+s\left(1-\theta\right)T_{\max}/2}\right)\left(\frac{1-s\theta T_{\max}\,\beta/2}{1+s\theta T_{\max}\,\beta/2}\right)
\end{aligned}\qquad(3)$$

In order to represent an uncertain system into the multiplicative form, suppose that the real system belongs to a family of plants Π and can be defined by using the following perturbation to the nominal plant G_0:

$$G(s)=\left(1+\Delta(s)W_m(s)\right)G_0(s),\quad \forall G(s)\in\Pi \qquad(4)$$

In this equation, $W_m(s)$ is a stable transfer function introducing the upper bound of the uncertainty and "(*s*) indicates the admissible uncertainty block, with "(*s*) „<1. Achieving the $W_m(s)$ involves some numerical searches in the frequency domain so that (5) is supported.

$$\begin{aligned}
&\frac{G(j\omega)}{G_O(j\omega)}-1=\Delta(j\omega)W_m(j\omega)\\
&\left|\frac{G(j\omega)}{G_O(j\omega)}-1\right|\le\left|W_m(j\omega)\right|\quad,\quad\forall\omega
\end{aligned}\qquad(5)$$

Hence, in order to utilize the robust control method, the second uncertain part in (3) can be expressed by the multiplicative uncertainty structure as (6).

$$\begin{aligned}
&\frac{1-s\theta T_{\max}\,\beta/2}{1+s\theta T_{\max}\,\beta/2}=1-\frac{s\theta T_{\max}\beta}{1+s\theta T_{\max}\,\beta/2}\\
&=1+W_{mT}(s)\Delta(s)
\end{aligned}\qquad(6)$$

W_{mT}(s) must be determined in a way that

$$\left|W_{mT}(j\omega)\right|>\left|\frac{j\omega\theta T_{\max}\beta}{1+j\omega\theta T_{\max}\,\beta/2}\right| \qquad(7.1)$$

Therefore, it is equal to (7.2).

$$W_{mT}(s)=\frac{s\theta T_{\max}}{1+s\theta T_{\max}/3.475} \qquad(7.2)$$

This formulation of the communication channel time-delay is depicted in fig. 3 and used in $H_{„}$ framework.

III. Controller Design

As it is mentioned before, the main goal of the suggested control scheme is to achieve transparency and stability of the system versus foregoing sources of instability. This is done by designing two local controllers; one is placed in the remote site (slave controller) denoted by C_s and the other one is sat in the local site (master controller) represented by C_m. The remote controller guarantees the position/velocity tracking while the local controller must preserve force tracking (transparency) and stability of the overall system.

In order to control the bilateral teleoperation system, new robust LMI-based PID controllers are established based on $H_{„}$ theory in both sites. In the suggested method, the PID controller is designed as a special case of the output-feedback controller and then convex optimization will be employed to find optimal parameters of the controllers for selected weighting functions. A plant with its related weighting function can be shown as the generalized structure depicted in fig. 4. The state space of the depicted plant is defined by (8).

In (8), u is the control input, w is a vector of exogenous signals (reference input signal, disturbance and sensor noise signals) and e is the measurement output signals whilst z is a

DOI: 01.IJRTET.9.1.513

vector of output signals ($(z_1\ z_2\ \dots\ z_j)^T$) related to the performance of the total system.

$$\begin{aligned} \dot{x} &= Ax + B_w w + Bu \\ z &= C_z x + D_{zw} w + D_z u \\ e &= Cx + D_w w \end{aligned} \tag{8}$$

The dynamical output-feedback controller will be illustrated with a state space realization given in (9) such that makes desired changes in the output vector.

$$\begin{aligned} \dot{\zeta} &= A_K \zeta + B_K e \\ u &= C_K \zeta + D_k e \end{aligned} \tag{9}$$

Furthermore, the state space realization of the closed-loop can be introduced by (10).

$$\left(\begin{array}{c|c} A' & B' \\ \hline C' & D' \end{array}\right) = \left(\begin{array}{cc|c} A + BD_k C & BC_k & B_w + BD_k D_w \\ B_k C & A_k & B_k D_w \\ \hline C_z + D_z D_k C & D_z C_k & D_{zw} + D_z D_k D_w \end{array}\right) \tag{10}$$

From bounded real lemma [26] $A2$ is stable and H_∞ norm of the desired channel between w_i and z_j in the augmented plant is smaller than γ if and only if there was a symmetric P such that (11) is met.

$$\begin{pmatrix} A'^T P + PA' & PB'_{w_i} & C'_{z_j} \\ B'^{\,T}_{w_i} P & -\gamma I & D'^{\,T}_{z_j w_i} \\ C'^{\,T}_{z_j} & D'_{z_j w_i} & -\gamma I \end{pmatrix} < 0 \ , \ P > 0 \tag{11}$$

Where B_{wi}, C_{zj} and D_{zjwi} are related to the desired input w_i and output z_j from the augmented plant in fig. 4. By employing the congruence transformation in the form of $diag(\Pi_1, I, I)$ [27] in which Π_1 must be introduced by (12). The none-convex problem in (11) can be converted to the convex problem with new parameters introduced in (13) via exerting congruence transformation of (12) and will be applied in theorem1.

$$\Pi_1 := \begin{pmatrix} X & I \\ M^T & 0 \end{pmatrix}, \ \Pi_2 := \begin{pmatrix} I & Y \\ 0 & N^T \end{pmatrix}, \ P\Pi_1 = \Pi_2 \tag{12}$$

In (12), N and M are nonsingular matrices that must satisfy $MN^T = I - XY$.

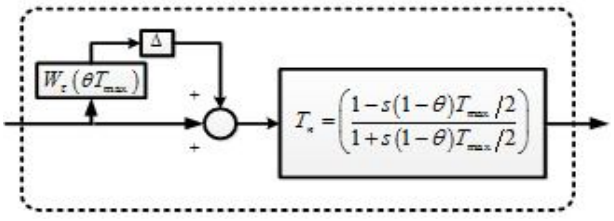

Figure 3. Schematic of the uncertain time-delay

$$\begin{aligned} \hat{A}_k &:= \begin{pmatrix} NA_k M^T + NB_k CX + \\ YBC_k M^T + Y\left(A + BD_k C\right) X \end{pmatrix} \\ \hat{B}_k &:= NB_k + YBD_k \\ \hat{C}_k &:= C_k M^T + D_k CX \\ \hat{D}_k &:= D_k \end{aligned} \tag{13}$$

In the next subsections, design of the local controllers will be described based on the foregoing principles.

A. LMI based robust PID controller design

The considered local systems with their controllers have to be stated as the structure in fig. 5.

In fig. 5 W_{mi} is the uncertainty weighting function due to variations in the dynamics of the slave manipulator and remote environment or change in time-delay which can be achieved from (5). W_{pi}, W_{ui} are the performance and controller weighting functions and will be chosen based on the objectives of the controller design in both sites. In order to design the performance weighting function the characteristics of the desired output in both frequency or time domain (like cut off frequency or settling time or maximum overshoot) should be constructed in the frequency domain and so the desired transfer function of the system will be established from these characteristics [28]. Concerning the nominal performance condition $\|W_{pi}(j\omega)S_i(j\omega)\|_\infty < 1$ from robust control theory, W_{pi} will be achieved. Also in order to design W_{ui} by considering the bounded effect on the controller signal namely $\|W_{ui}(j\omega)f_i(j\omega)\|_\infty < 1$, W_{ui} can be constructed from the same method as W_{pi}. Where $i=m, s$ referring to the master and slave sites. Then for $i=s$:

$$G_s'(s) = G_s(s) \big/ \left(1 + Z_e G_s(s)\right) \tag{14}$$

$G_s(s)$ and Z_e are introduced before. In fact, equation (14) introduces the transfer function of Y_s/F_s in fig. 2, and must be employed in design of C_s that is meant to support the position tracking of the slave system. Moreover, for $i=m$:

$$G_m'(s) = G_m(s) \frac{C_s(s) G_s(s) Z_e}{1 + G_s(s) Z_e + C_s(s) G_s(s)} T_n(s) \tag{15}$$

This comes from the Closed-loop formation of the slave site with its designed controller. As the master controller is considered to guarantee force tracking as well as stability of the overall system, the transfer function of F_r/F_m must be used to meet these objectives. Therefore, by using the structure of fig. 3 instead of communication time-delay, (15) has to be used in addition to W_{mT} which is connected with variation of time-delay.

So the procedure of controller design for this structure includes two regular step: at the first step a controller is designed for the slave site ($i=s$) with related weighting functions and then by transmitting the slave Closed-loop to the local site the master controller will be established ($i=m$).

The structure depicted in fig. 5 could be shown as the augmented plant illustrated in fig. 4. The conventional LMI based H_∞ output-feedback controller will be achieved from theorem1 [27].

Theorem1: Position tracking for the slave and master systems against the uncertainty in parameters of the slave system, remote environment, and time-delay could be supported if there were X and Y for the following minimization LMI.

DOI: 01.IJRTET.9.1.513

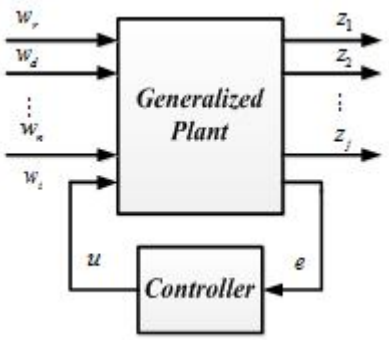

Figure 4. Schematic of the augmented plant

$$\text{mininmize } \gamma$$

$$\text{Subject to: } \begin{pmatrix} \Pi_{11} & \Pi_{12} & \Pi_{13} & \Pi_{14} \\ \Pi_{21} & \Pi_{22} & \Pi_{23} & \Pi_{24} \\ \Pi_{31} & \Pi_{32} & -\gamma I & \Pi_{34} \\ \Pi_{41} & \Pi_{42} & \Pi_{43} & -\gamma I \end{pmatrix} < 0 \qquad (16)$$

$$\begin{pmatrix} X & I \\ I & Y \end{pmatrix} > 0$$

$$\Pi_{11} := AX + XA^T + B\hat{C}_k + \left(B\hat{C}_k\right)^T$$

$$\Pi_{22} := A^T Y + YA + B\hat{C}_k + \left(B\hat{C}_k\right)^T$$

$$\Pi_{21} := \hat{A}_k + \left(A + B\hat{D}_k C\right)^T$$

$$\Pi_{31} := \left(B_{w_i} + B\hat{D}_k D_{w_i}\right)^T$$

$$\Pi_{32} := \left(YB_{w_i} + \hat{B}_k D_{w_i}\right)^T$$

$$\Pi_{43} := D_{z_j w_i} + D_{z_j}\hat{D}_k D_{w_i}$$

$$\Pi_{41} := C_{z_j} X + D_{z_j}\hat{C}_k$$

$$\Pi_{42} := C_{z_j} + D_{z_j}\hat{D}_k C$$

The LMIs of (16) are achieved from (11) by using congruence transformation introduced in (12).

In (16), $\Pi_{ij}=\Pi_{ji}^T$, and $A, B_{wi}, C_{zj}, D_{zjwi}$ are introduced before, whereas A_k, B_k, C_k represent transformed parameters of the controller of (13) which are used in order to preserve linearization of the problem. The real parameters of the controller can be constructed from the relations in (17).

$$\begin{aligned} D_k &:= \hat{D}_k \\ C_k &:= \left(\hat{C}_k - D_k CX\right) M^{-T} \\ B_k &:= N^{-1}\left(\hat{B}_k - YBD_k\right) \\ A_k &:= N^{-1}\left(\hat{A}_k - NB_K CX - YBC_k M^T - Y\left(A + BD_k C\right)X\right) M^{-T} \end{aligned} \qquad (17)$$

So next, in order to design a robust PID controller, the PID controller design problem should be put into the output-feedback controller structure and then the extended theorem2 can be used to establish the robust PID controller. A PID controller signal is founded by (18).

$$u(t) = \begin{pmatrix} K_p & K_I & K_D \end{pmatrix}\begin{pmatrix} e & \int e & e' \end{pmatrix}^T \qquad (18)$$

Converting e into $e_o=(e$ +"e $e2)^T$ in the augmented plant, the new PID-augmented plant shown in fig. 6 is established and the problem of PID controller design can be shown as a special case of the output-feedback controller. So the state space of the augmented plant is transformed into (19).

$$\begin{aligned} \dot{\tilde{x}} &= \tilde{A}\tilde{x} + \tilde{B}_w w + \tilde{B}u \\ z &= \tilde{C}_z \tilde{x} + D_{zw} w + D_z u \\ e_o &= \tilde{C}\tilde{x} + \tilde{D}_w w \end{aligned} \qquad (19)$$

Where xB is achieved from (20).

$$\begin{aligned} x_{n+1} &= \int e \to \dot{x}_{n+1} = e = \begin{pmatrix} C & 0 \end{pmatrix}\tilde{x} + D_w w \\ &\to \tilde{x} = \begin{pmatrix} x & x_{n+1} \end{pmatrix}^T \end{aligned} \qquad (20)$$

From (8) and (19) AB, CB_z, BB_w, BB is represented by (21).

$$\tilde{A} = \begin{pmatrix} A & 0 \\ C & 0 \end{pmatrix},\ \tilde{C}_z = \begin{pmatrix} C_z & 0 \end{pmatrix},$$
$$\tilde{B}_w = \begin{pmatrix} B_w \\ D_w \end{pmatrix}, \tilde{B} = \begin{pmatrix} B \\ 0 \end{pmatrix} \qquad (21)$$

And regarding:

$$\begin{aligned} e &= \begin{pmatrix} C & 0 \end{pmatrix}\tilde{x} + D_w w \to \\ \dot{e} &= \begin{pmatrix} C & 0 \end{pmatrix}\tilde{A}\tilde{x} + \begin{pmatrix} C & 0 \end{pmatrix}\tilde{B}_w w + \begin{pmatrix} C & 0 \end{pmatrix}\tilde{B}u \\ &\xrightarrow{(C\ \ 0)\tilde{B}=0} \dot{e} = \begin{pmatrix} C & 0 \end{pmatrix}\tilde{A}\tilde{x} + \begin{pmatrix} C & 0 \end{pmatrix}\tilde{B}_w w, \\ \int e &= x_{n+1} = \begin{pmatrix} 0 & \cdots & 0 & 1 \end{pmatrix}\tilde{x} \end{aligned} \qquad (22)$$

CB, DB_w are introduced by (23).

$$e_o = \begin{pmatrix} e & \int e & e' \end{pmatrix}^T \to \tilde{C} = \begin{pmatrix} C & 0 \\ 0 & 1 \\ CA & 0 \end{pmatrix},\ \tilde{D}_w = \begin{pmatrix} D_w \\ 0 \\ CB_w \end{pmatrix} \qquad (23)$$

So by forming the new augmented plant from (21) and (23) the transfer function between an especial input w_i and output z_j can be represented by (24).

$$T_{z_j w_i} = \left(\begin{array}{c|c} A'' & B'' \\ \hline C'' & D'' \end{array}\right) = \left(\begin{array}{cc|c} \tilde{A} + \tilde{B}D_K\tilde{C} & \tilde{B}C_K & \tilde{B}_{w_i} + \tilde{B}D_K\tilde{D}_{w_i} \\ B_K\tilde{C} & A_k & B_K\tilde{D}_{w_i} \\ \hline \tilde{C}_{z_j} + \tilde{D}_{z_j}D_K\tilde{C} & \tilde{D}_{z_j}C_K & \tilde{D}_{z_j w_i} + \tilde{D}_{z_j}D_K\tilde{D}_{w_i} \end{array}\right) \qquad (24)$$

DOI: 01.IJRTET.9.1.513

Although A_k, B_k, C_k will be achieved for the new structure of the PID-augmented plant from therom2, by considering the applied structure and regarding that $D_k = (k_P \ k_I \ k_D)$, the coefficient of D_k will be enough to guarantee stability and performance of the system.

Regarding the new parameters, an extended version of theorem 1 can be used to design a robust PID controller.

Theorem 2. A robust PID controller could support the tracking performance (either position or force) and stability of the system if there were $\tilde{X}$, $\tilde{Y}$ for the following convex LMIs.

$$\text{mininmize } \gamma$$

$$\text{Subject to: } \begin{pmatrix} \Lambda_{11} & \Lambda_{12} & \Lambda_{13} & \Lambda_{14} \\ \Lambda_{21} & \Lambda_{22} & \Lambda_{23} & \Lambda_{24} \\ \Lambda_{31} & \Lambda_{32} & -\gamma I & \Lambda_{34} \\ \Lambda_{41} & \Lambda_{42} & \Lambda_{43} & -\gamma I \end{pmatrix} < 0 \qquad \begin{pmatrix} \tilde{X} & I \\ I & \tilde{Y} \end{pmatrix} > 0 \tag{25}$$

In (25), $\Lambda_{ij} = \Lambda_{ji}^T$ and other parameters are introduced in (26).

$$\begin{aligned} \Lambda_{11} &:= \tilde{A}\tilde{X} + \tilde{X}\tilde{A}^T + \tilde{B}\hat{C} + \left(\tilde{B}\hat{C}\right)^T \\ \Lambda_{22} &:= A^T\tilde{Y} + \tilde{Y}A + \tilde{B}\hat{C} + \left(\tilde{B}\hat{C}\right)^T \\ \Lambda_{21} &:= \hat{A}_k + \left(\tilde{A} + \tilde{B}\hat{D}\tilde{C}\right)^T \\ \Lambda_{43} &:= \tilde{D}_{z_j w_i} + \tilde{D}_{z_j}\hat{D}\tilde{D}_{w_i} \\ \Lambda_{32} &:= \left(\tilde{Y}\tilde{B}_{w_i} + \hat{B}\tilde{D}_{w_i}\right)^T \\ \Lambda_{31} &:= \left(\tilde{B}_{w_i} + \tilde{B}\hat{D}\tilde{D}_{w_i}\right)^T \\ \Lambda_{41} &:= \tilde{C}_{z_j}\tilde{X} + \tilde{D}_{z_j}\hat{C} \\ \Lambda_{42} &:= \tilde{C}_{z_j} + \tilde{D}_{z_j}\hat{D}\tilde{C} \end{aligned} \tag{26}$$

Proof. The new congruence transformation can be introduced by (27)

$$\Theta_1 := \begin{pmatrix} \tilde{X} & I \\ M^T & 0 \end{pmatrix}, \ \Theta_2 := \begin{pmatrix} I & \tilde{Y} \\ 0 & N^T \end{pmatrix}, \ P\Theta_1 = \Theta_2 \tag{27}$$

$N\text{Þ}$ and $M\text{Þ}$ are nonsingular matrices with proper dimension that must satisfy $M\text{Þ}N\text{Þ}^T = I - X\text{Þ}Y\text{Þ}$

Now applying $diag(\Theta_1, I, I)$ to (11) will end up in (28).

$$\begin{pmatrix} \Theta_1^T & & 0 \\ & I & \\ 0 & & I \end{pmatrix} \begin{pmatrix} A''^T P + PA'' & PB'' & C''^T \\ B''^T P & -\gamma I & D''^T \\ C'' & D'' & -\gamma I \end{pmatrix} \begin{pmatrix} \Theta_1 & & 0 \\ & I & \\ 0 & & I \end{pmatrix} < 0 \tag{28}$$

$$\rightarrow \begin{pmatrix} \Theta_1^T A''^T \Phi_2 + \Theta_2^T A'' \Theta_1 & \Theta_2^T B'' & \Theta_1^T C''^T \\ B''^T \Theta_2 & -\gamma I & D''^T \\ \Theta_1^T C''^T & D'' & -\gamma I \end{pmatrix} < 0$$

$$\Theta_1^T P \Theta_1 > 0$$

Now considering (24) and (27) theoem2 will be achieved so that the relation between the real parameters of the controllers and the converted ones are represented by (29).

$$\begin{aligned} \hat{A} &:= \begin{pmatrix} \tilde{N}\tilde{A}_k\tilde{M}^T + \tilde{N}\tilde{B}_k\tilde{C}\tilde{X} + \\ \tilde{Y}\tilde{B}\tilde{C}_k\tilde{M}^T + \tilde{Y}\left(\tilde{A} + \tilde{B}\tilde{D}_k\tilde{C}\right)\tilde{X} \end{pmatrix} \\ \hat{B} &:= \tilde{N}\tilde{B}_k + \tilde{Y}\tilde{B}\tilde{D}_k \\ \hat{C} &:= \tilde{C}_k\tilde{M}^T + D_k\tilde{C}\tilde{X} \\ \hat{D} &:= D_k \end{aligned} \tag{29}$$

Guaranteeing the system stability requires an additional constraint $D_k > 0$ which is added to the constraints of the theorem1. As D_k is equal to the coefficient of the PID controller this constraint supports the positivity of the parameters of the controller and therefore, stabilization of the designed controller

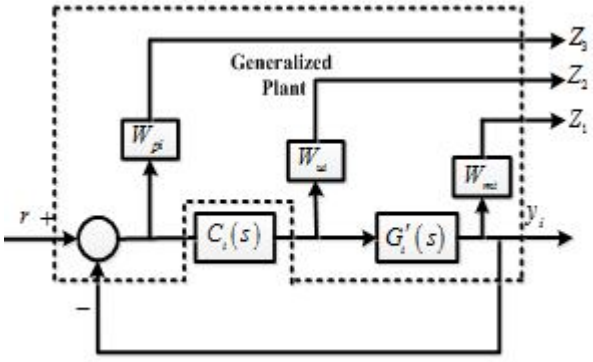

Figure 5. Slave and master sites with weighting functions

B. LMI based multiobjective H_2/H_∞ controller design

Standard structure of fig. 5 can be shown as the generalized plant depicted in fig. 4, and from the generalized plant a conventional multiobjective H_2/H_∞ controller can be constructed from theorem3.

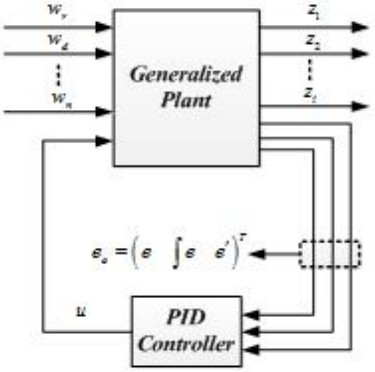

Figure 6. Schematic of the PID-augmented plant

DOI: 01.IJRTET.9.1.513

Theorem3. By considering uncertainty in the communication channels and accompanied noise with reflected force (received from the remote environment via the backward communication channel), force tracking (transparency) can be achieved by using a multiobjective H_2/H_∞ controller in the master site. So a multiobjective H_2/H_∞ controller with tracking error bound γ exists if there were X and Y that would satisfy the minimization linear matrix inequality in theorem1 with following additional constraints:

$$\begin{pmatrix} \Pi_{11} & \Pi_{12} & \Pi_{13} \\ \Pi_{21} & \Pi_{22} & \Pi_{23} \\ \Pi_{31} & \Pi_{32} & -I \end{pmatrix} < 0,$$
$$\begin{pmatrix} X & I & M_{13} \\ I & Y & M_{23} \\ M_{31} & M_{32} & Q \end{pmatrix} > 0, \qquad (30)$$
$$Tr(Q) < \nu,\ D_{z_j w_i} + D_{z_j} \hat{D}_k D_{w_i} = 0$$

Where $\Pi_{11}, \Pi_{21}, \Pi_{31}, \Pi_{22}, \Pi_{32}$ are introduced before and:

$$M_{31} := C_{z_j} X + D_{z_j} \hat{C}_k$$
$$M_{32} := C_{z_j} + D_{z_j} \hat{D}_k C \qquad (31)$$

And the real parameters of the Controller can be constructed from (17).

Proof. By considering the introduced state space representation of the system, H_2 norm of the system will be smaller than ν if there was a P which satisfies LMIs in (32)

$$D_{w_i} = 0, \begin{pmatrix} A'^T P + PA'^T & PB_{w_i}' \\ B_{w_i}'^T P & -I \end{pmatrix} \prec 0,$$
$$\begin{pmatrix} P & C_{z_j}^T \\ C_{z_j}' & Q \end{pmatrix} \succ 0, \qquad (32)$$
$$trace(Q) < \nu$$

In (32), Q is an auxiliary parameter applied to maintain linearization. By using the transformation of (12) it can be converted to (30) and will be added to the constraints of theorem1 to design a multiobjective H_2/H_∞ controller.

IV. Simulation Results

In order to show the effectiveness of the proposed method the simulation result of a teleoperation system with parameters of Table. 1 will be analyzed.

Considering the changes of the slave parameters in table.1 the multiplicative uncertainty weighting function for the slave manipulator and time-delay of communication channels can be obtained from (5).

$$W_{ms}(s) = 18.05(s+1.035)/(s+5.499)$$
$$W_{mm}(s) = W_{mT}(s) = 1.5s/(0.4329s+1) \qquad (33)$$

Table I. Parameters Of System

Components	Values	COMPONENTS	values
M_m(Kg)	1.5	T_{min}	0
B_m(N/m)	11	T_{max}	3
$M_{s\_}$	0.1	θ	0.5
M_s^-	3.9	$Z_{e\_}$	1
$B_{s\_}$	3	Z_e^-	3
B_s^-	27	K_p, k_f	1,1

The bode diagrams of fig .7 show that the uncertainty weighting functions resulted from the changes in time-delay of communication channels and parameters of the slave site, cover the modified range of variations in parameters.

So with notion the uncertainty weighting function of the slave site for the generalized plant with $W_{us}=0.0008$ (to restrict the maximum controller output to below 3), and $W_{ps}=5/(s+0.001)$ (in order to have the slave position without steady state error and fast time response), the robust PID controller (34) has been achieved from extended theorem2 by using numerical computations of the mincx solver in Matlab toolbox that support the tracking performance.

$$C_s(t) = \begin{pmatrix} 33.9381 & 5.8247 & 5.898\times10^{-4} \end{pmatrix} E_s(t)$$
$$E_s(t) = \begin{pmatrix} e_s(t) & \int e_s(\tau)d\tau & e_s'(t) \end{pmatrix}^T \qquad (34)$$

By employing shown structure in fig. 5 and $W_{um}=0.2$ (in order to restrict controller input bellow 5), $W_{pm}=1/(s+10^{-5})$ (to impose the desired time response to the output of the master manipulator with lower settling time and without steady state error), the generalized structure of fig. 6 has been used in theorem1 in order to reach the tracking performance with robustness against time-delay in communication channel.

$$C_m(t) = \begin{pmatrix} 0.9277 & 2.5221\times10^{-5} & 0.7931 \end{pmatrix} E_m(t)$$
$$E_m(t) = \begin{pmatrix} e_m(t) & \int e_m(\tau)d\tau & e_m'(t) \end{pmatrix}^T \qquad (35)$$

Where $e_s(t)=y_m(t-T_{ms})-y_s(t)$ and $e_m(t)=f_h(t)-f_e(t-T_{sm})$. On the other hand by using theorem2 and applying Normalized Coprime Factorization (NCF) method, the first 8th order multiobjective H_2/H_∞ controller will be reduced to the following 4th order controller for the master site introduced by (36).

$$C_m = \left(\begin{array}{cccc|c} -3.923\times10^{-5} & -0.2186 & 0.0065 & 0.0119 & 0 \\ 0 & -1.64 & 3.625 & 0 & 0 \\ 0 & -3.625 & -1.64 & 1.907 & 0 \\ 0 & 0 & 0 & -5.903 & 8 \\ \hline 0.0238 & -3.645 & 1.094 & 1.996 & 0 \end{array}\right) \qquad (36)$$

Time response of the teleoperation system with designed controllers for nominal values of the parameters and time-delay are shown at fig. 8 to fig. 12.

Simulation results show the responses of the system for the input signals that is usually used in such systems. As it can be seen from fig. 8 to fig. 12 the designed robust PID

DOI: 01.IJRTET.9.1.513

controller has a faster time response rather than the multiobjective H_2/H_∞ controller while the control effort is acceptable. On the other hand, the PID controller cannot reject measurement noise that imposes more control effort to this controller.

Since the simulation results show the responses of the system for the nominal value of the parameters μ analysis has been applied to test the stability and performance of the system for different values of the parameters.

The last two figures of this section indicate the stability and performance statuses based on the μ analysis. Since the values of the μ bound related to the stability of the system is smaller than one and for performance is near one, the designed controllers preserve the global stability regardless the uncertainty in dynamics of the slave manipulator and variable time-delay in communication channel while the performance of the system do not change seriously.

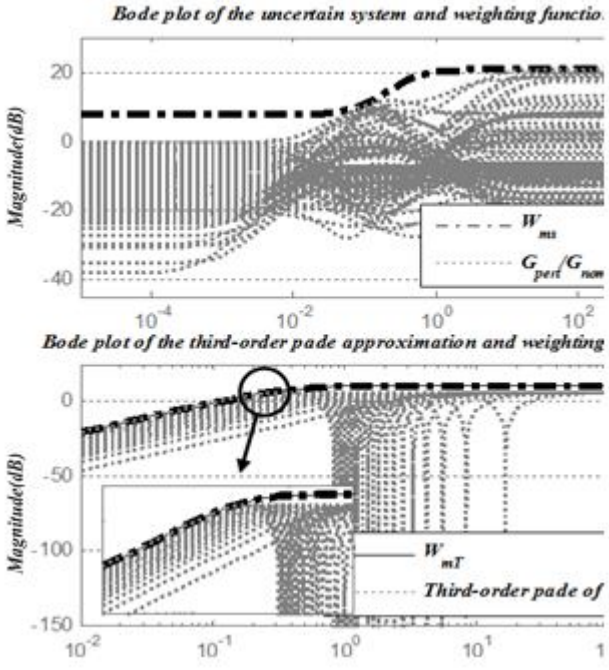

Figure 7. The bode diagram of the W_{ms} and G/G_0-*1* and bode diagram of the W_{mT} and approximation of time-delay

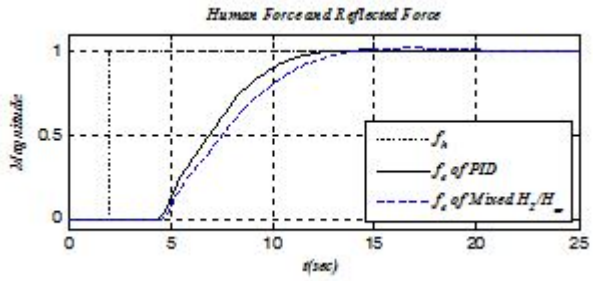

Figure 8a. Human operator and Reflected forces

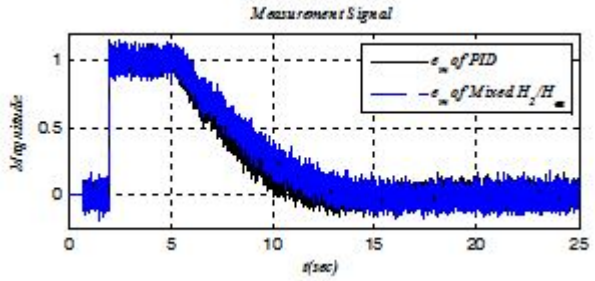

Figure 8b. Measurement signal ($e_m(t)$)

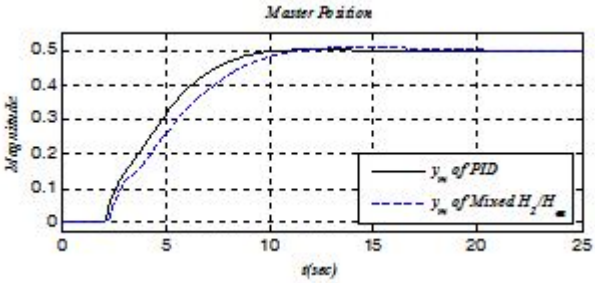

Figure 9a. Position of master manipulators ($y_m(t)$)

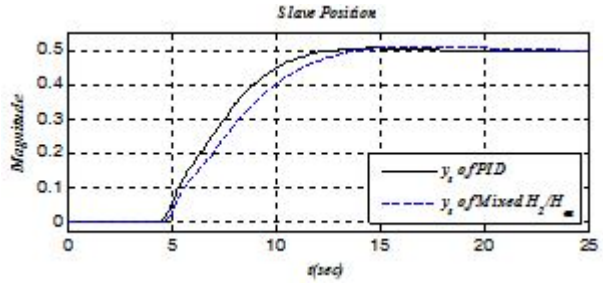

Figure 9b. Position of slave manipulators ($y_s(t)$)

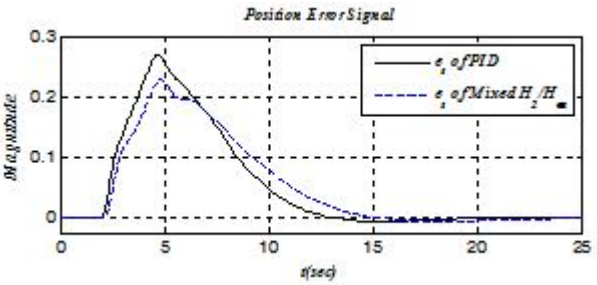

Figure 9c. Position error signals ($e_s(t)$)

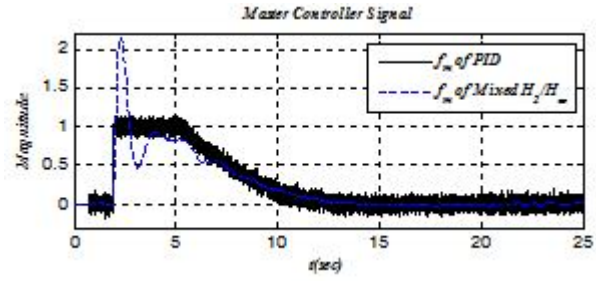

Figure 10a. Master controller signal ($f_m(t)$).

DOI: 01.IJRTET.9.1.513

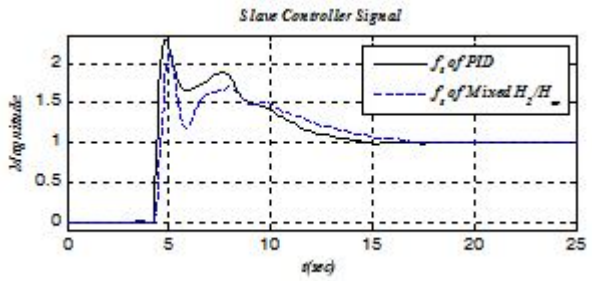

Figure 10b. Slave controller signal ($f_s(t)$)

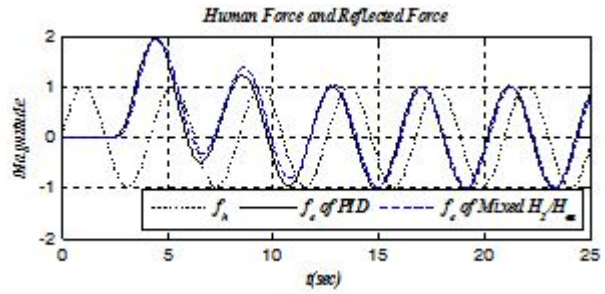

Figure 11a. Human operator and Reflected forces for sinusoid input with 1 rad/sec frequency

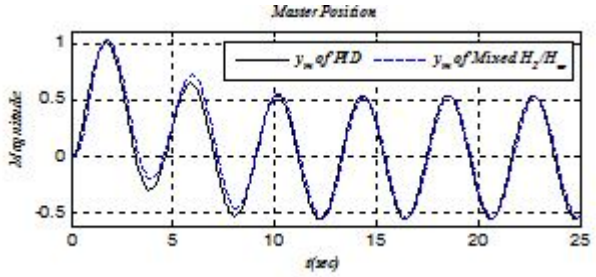

Figure 11b. Position of master manipulators ($K_p y_m(t)$) for Kp=4.1, Kf=0.25

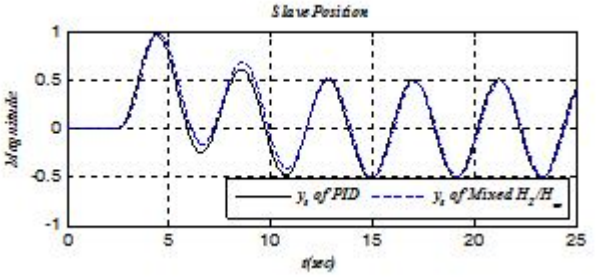

Figure 11c. Position of slave manipulators ($y_s(t)$)

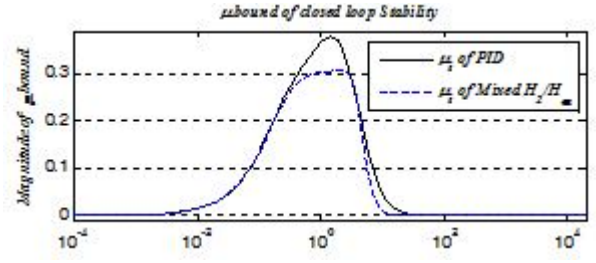

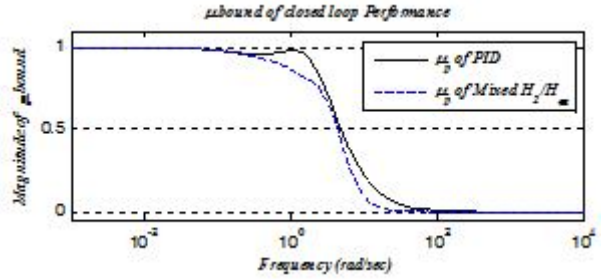

Figure 12a. ì bound of Closed-loop stability and performance with designed controller

Conclusions

Due to the transmission time-delay in communication channel, it is fairly difficult to ensure the Closed-loop stability of a teleoperation system, so major concerns of the controller design for a bilateral teleoperation system are preserving the stability and transparency of the teleoperation system despite the time-delay in communication channels. In this paper a new robust PID controller has been proposed by applying a Linear Matrix Inequality approach in order to guarantee complete transparency against the variable time-delay with known upper bound and the uncertainty in parameters of the slave manipulator and remote environment. Two separated controllers have been established to ensure the complete transparency and stability of the Closed-loop. In order to show the effectiveness of the proposed method, the simulation results for both multiobjective H_2/H_∞ and robust H_∞ PID controllers in master site have been shown, while the slave controller was a robust PID controller in both situations. It can be seen from the simulation results that the robust PID controller shows acceptable results in comparison with the multiobjective H_2/H_∞ controller. Furthermore, the PID controller has more practical applications. Although the designed PID controller cannot reduce the effects of the measurement noise, in many practical cases the manipulators have the low frequency characteristics, consequently it does not effect on the final response of the system intensely. In the following researches the noise reduction can be added to the robust PID controller by using some stochastic calculations to reduce the control efforts of such controllers.

References

[1] D.A. Lawrence, "Stability and transparency in bilateral teleoperation," *IEEE Transaction on Robotics and Automation*, vol. 9, no. 5, pp. 2649-2655, 1993.

[2] A. Smith and K. Hashtrudi-Zaad, "Smith-predictor based predictive control architectures for time-Delayed teleoperation systems," *International Journal of Robotics Research*, vol. 25, no. 8, pp. 797-818, 2006.

[3] A. Sano, H. Fujimoto and T. Takai, "Network-based force-reflecting teleoperation," *IEEE International Conference on Robotics and Automation*, pp. 3126-3131, 2000.

[4] S. Ganjefar, H. Momeni and F. Janabi-Sharifi, "Teleoperation systems design using augmented wave variables and smith predictor method for reducing time-delay effects," *IEEE International Symposium on Intelligent Control*, pp. 333-338, 2002.

DOI: 01.IJRTET.9.1.513

[5] M. Boukhnifer and A. Ferreira, "H_2 optimal controller design for micro-teleoperation with delay," *International Conference on Intelligent Robots and Systems*, pp. 224-229, 2004.

[6] K. Hosseini-Sunny, H. Momeni and F. Janabi-Sharifi, "Adaptive teleoperation systems design," *IEEE Conference on Control Applications*, pp. 334-339, 2005.

[7] S. Ganjefar and M. Mir, "Optimal control design in teleoperation systems for reducing time-delay effects," *International Conference on Control, Automation and Systems*, pp. 2447-2441, 2007.

[8] M. Sha-Sadeghi, H. Momeni, R. Amirifar, S. Ganjefar , "A new adaptive inverse control scheme for teleoperation system with varying time-delay," *IEEE Conference on Control Applications*, pp. 199-204, 2006.

[9] S. Sirouspour, A. Shahdi, "Model predictive control for transparent teleportation under communication time-delay," *IEEE Transactions on Robotics*, vol. 22, no. 6, 2006.

[10] M. Tavakoli, A. Aziminejad, R. V. Patel, M. Moallem, "Discrete-time bilateral teleoperation: modeling and stability analysis," *IET Control Theory Appl.*, Vol. 2 n. 6, pp. 496–512, 2008.

[11] R. Moreau, M. T. Pham, M. Tavakoli, M. Q. Le, T. Redarce, "Sliding-Mode Bilateral Teleoperation Control Design for Master-Slave Pneumatic Servo Systems," *IFAC Control Engineering Practice*, Vol. 20 n. 6, pp. 584-597, 2012.

[12] K. Hosseini Suny, H. Momeni, F. Janabi-Sharifi, "A modified adaptive controller design for teleoperation systems", *Robotics and Autonomous Systems*. 58, 676-683 2010.

[13] X. Liu, M. Tavakoli, "Adaptive Inverse Dynamics Four-Channel Control of Uncertain Nonlinear Teleoperation Systems," *Advanced Robotics*, Vol. 25, pp. 1729–1750, 2011.

[14] F. Coutinhoa, R. Cortesao, "Adaptive stiffness estimation for compliant robotic manipulationusing stochastic disturbance models," *International Journal of Systems Science*, Vol. 42, n.8, pp. 241–1252, 2011.

[15] Z. Li, Y. Xia, "Adaptive neural network control of bilateral teleoperation with unsymmetrical stochastic delays and unmodeled dynamics," International Journal of Robust and Nonlinear Control, 2013.

[16] A. Nikoobin, R. Haghighi, "Lyapunov-based nonlinear disturbance observer for serial n-link robot manipulators," Journal of Intelligent and Robotic Systems, vol. 55, no. 2-3, pp. 135–153, 2009.

[17] K. Natori, T. Tsuji, K. Ohnishi, "Time-Delay Compensation by Communication Disturbance Observer for Bilateral Teleoperation Under Time-Varying Delay," *IEEE Transactions on Industrial Electronics*, Vol. 57, no. 3, pp. 1050–1062, 2010.

[18] A. Mohammadi, M. Tavakoli, H. J. Marquez, "Disturbance observer based control of nonlinear haptic Teleoperation systems," *IET Control Theory and Application*, Vol. 5, no. 17, pp. 2063–2074, 2011.

[19] K. Gu, V.L. Kharitonov, J. Chen, "Stability of Time-Delay Systems," Springer, 2003.

[20] M. ShaSadeghi, H.R. Momeni, R. Amirifar, "H_2 and L_1 control of a teleoperation system via LMIs," *Applied Mathematics and Computation*, vol. 206, pp. 669–677, 2008.

[21] Hua and P. X. Liu, "Convergence analysis of teleoperation systems with unsymmetric time-varying delays," *IEEE Transactions on Circuits and Systems-II: Express Briefs*, vol. 56, no. 33, pp. 240-243, 2009.

[22] A. Alfi and M. Farrokhi, "A simple structure for bilateral transparent teleoperation systems with time-delay," *ASME Journal of Dynamic Systems, Measurement and Control*, vol. 130, no. 4, 2008.

[23] P. F. Hokayem and M. W. Spong, "Bilateral teleoperation: an historical survey," *Automatica*, vol. 42, pp. 2035-2055, 2006.

[24] J. Filipiak, "Modeling and Control of Dynamic Flows in Communication Networks," Berlin, Germany, Springer-Verlag, 1988.

[25] Tipsuwan Yodyium, Chow Mo-Yuen, "Control Methodologies in Networked Control Systems," *Control Engineering Practice*, vol. 10, 2003, pp. 1099-1111.

[26] S. Boyd, L. El Ghaoui, E. Feron, V. Balakrishnan, Linear Matrix Inequalities in Systems and Control Theory, PA: SIAM, Philadelphia, 1994.

[27] C. Scherer, P. Gahinet P. and M. Chilali, "Multiobjective output-feedback control via LMI optimization," *IEEE Transactions on Automatic Control*, vol. 42, no. 7, 1997.

[28] J. Hu, C. Bohn, H.R. Wu, "Systematic H_{∞} weighting function selection and its application to the real-time control of a vertical take-off aircraft," *Control Engineering Practice*, Vol. 8, pp. 241-252, 2000.

DOI: 01.IJRTET.9.1.513